

Higher-Order QCD prediction for dark matter pair associated with a b-jet production at the LHC

Li Gang^{a,*}, Yu Si-He^a, Song Mao^a, Zhang Yu^b, Zhou Ya-Jin^c, and Guo Jian-You^a

^a *School of Physics and Material Science,
Anhui University, Hefei, Anhui 230039, P.R.China*

^b *School of Physics, Nanjing University,
Nanjing, Jiangsu 210093, P.R.China and*

^c *School of Physics, Shandong University,
Jinan Shandong 250100, P.R. China*

(Dated: November 21, 2016)

Abstract

Dark matter associated visible particle production at high energy colliders provides a unique way to determine the microscopic properties of the dark matter. We investigate a pair of fermionic dark matter particles associated with a b-jet production at the LHC, through a mediator which couples to standard model or dark matter particles via either a vector or axial-vector coupling. The calculation is performed by implementing these simplified models in the FeynRules/MadGraph5 aMC@NLO framework. In our calculation, next-to-leading order QCD corrections and parton-shower effects are considered. We find that this process has a sizeable cross section and the QCD correction can reach more than 2 times than LO results. We also investigate the discovery potential in several benchmark scenarios at the 13TeV LHC.

* lig2008@mail.ustc.edu.cn

I. INTRODUCTION

The astrophysical and cosmographic observational evidences have confirmed the existence of dark matter (DM) and provided the DM density in our universe [1]. However, these observations don't tell us the information about the mass of DM particle or whether it interacts with the Standard Model (SM) particles. Determining the nature of DM particle quantitatively is one of the most important tasks both in cosmology and particle physics. Among all the DM candidates, weakly interacting massive particles (WIMPs) is the most compelling one. This is due to that it offers the possibility to understand the relic abundance for the DM as a natural consequence of the thermal history of the universe [2]. Some extensions of the SM, such as Supersymmetry [3, 4], Universal Extra Dimensions [5] or Little Higgs Models [6, 7], naturally lead to good candidates for WIMPs and the cosmological requirements for the WIMP abundance in the universe. However, all of these theories still lack experimental support, and it is difficult to judge which theory is proper for the DM particle. Additionally, the first observation of the DM may come from direct- or indirect-detection experiments, which is difficult to provide information about the general properties of the DM particle. Thus, model-independent studies of DM phenomenology are particularly important.

There are many experiments currently running or planned aiming to test the hypothesis by searching for WIMPs. These experiments can be divided into two classes: direct detection experiments, which search for the scattering of dark matter particles off atomic nuclei within a detector, such as CDMS, XENON, LUX, PandaX; and indirect detection experiments, which look for the products of WIMP annihilations, such as Fermi Gamma-ray Space Telescope, PAMELA. An alternative approach to the detection of WIMPs in nature is to produce them at high energy colliders. Experiments with the Large Hadron Collider (LHC) may be able to detect WIMPs produced in collisions of the LHC proton beams. Because a WIMP has negligible interactions with matter, it will may not be detected as missing energy and momentum which escapes the LHC detectors, the useful method is searching the DM particle production associated a visible particle, such as jet, gauge boson, heavy quark.

Recently, some observational results favour a light DM with a mass around 10 GeV in various experiments. The DAMA experiment has reported a signal of annual modulation at a highly significant level [8], which is consistent with a discovery interpretation from a low

mass dark matter in direct measurements by CoGeNT [9], CRESST [10] and CDMS [11] experiments. While this region of parameter space is excluded by the other experiments like XENON100 [12], LUX [13] and SuperCDMS [14]. In order to clarify this puzzle, there have been more researches in light DM models (where the DM mass is order of a few GeV) [15–24].

In the case of a WIMP, stability on the order of the lifetime of the universe implies that pair production must highly dominate over single production, and precludes the WIMP from decaying within the detector volume. Searches for dark matter in missing momentum channels can be classified based on the visible particles against which the invisible particles recoil. Existing experimental studies have considered the cases in which the visible radiation is a jet of hadrons (initiated by a quark or gluon) [25–27], a photon [28, 29], or a W/Z boson decaying into leptons or hadronic jets [30–32]. The bottom quark can be identified by reconstructing secondary vertices, and the high- p_T bottom quark can be tagged with reasonably high efficiency at the LHC, meanwhile the observation of a bottom quark with high- p_T can reduce the backgrounds of the dark matter production. Thus, it is very interesting to study the dark matter pairs associated with a (anti)bottom quark production at the LHC. Because the LHC is a proton-proton collider, the QCD correction should be considered for any process if someone wants to make a reliable prediction. More recently, the production of DM pairs plus a jet, photon and W/Z have been calculated to QCD next-to-leading order (NLO) [33–42]. In Ref.[43], the DM pairs associated with a bottom quark production at LO for scalar coupling have been studied. In this work, we investigate a pair of fermionic dark matter particles associated with a b-jet production up to QCD NLO in the simplified model at the LHC.

The paper is arranged as follows: in Section II we briefly describe the related simplified model and present the calculation strategy. In Section III, we present some numerical results and discussion. Finally, a short summary is given in Section IV.

II. SIMPLIFIED MODEL AND CALCULATION STRATEGY

We assume that the dark matter candidate is a new particle which is singlet under the SM local symmetries, and all SM particles are singlets under the dark-sector symmetries. The interactions between the SM and DM sectors are presumably effected by the exchange

of some heavy mediators, which could be a vector, axial vector or scalar particles. Given the assumption that the WIMPs are SM singlets, the factor in each operator consisting of SM fields must also be invariant under SM gauge transformations. The interactions between the DM and SM quarks are described by the simplified model in Refs[33, 39, 41].

In the framework of the simplified model, the interaction of a spin-1 vector or axial-vector mediator (Y_1) with a Dirac fermion DM (X_D) is given by

$$\mathcal{L}_{X_D}^{Y_1} = \bar{X}_D \gamma_\mu (g_{X_D}^V + g_{X_D}^A \gamma_5) X_D Y_1^\mu, \quad (1)$$

and with quarks by

$$\begin{aligned} \mathcal{L}_{\text{SM}}^{Y_1} = \sum_{i,j} \bigg[& \bar{d}_i \gamma_\mu (g_{d_{ij}}^V + g_{d_{ij}}^A \gamma_5) d_j \\ & + \bar{u}_i \gamma_\mu (g_{u_{ij}}^V + g_{u_{ij}}^A \gamma_5) u_j \bigg] Y_1^\mu, \end{aligned} \quad (2)$$

where u and d represent up- and down-type quarks, respectively. $g^{V/A}$ are the vector/axial-vector couplings of DM and quarks, and $i, j (i, j=1,2,3)$ are flavour indices. This notation are adopted to the actual implementation in FEYNRULES [44]. The model files can be downloaded at the FEYNRULES website [45].

The pure vector and pure axial-vector mediators are given by setting the parameters in the Lagrangians (1) and (2) to

$$g_{X_D}^V \equiv g_X \quad \text{and} \quad g_{X_D}^A = 0 \quad (3)$$

$$g_{u_{ii}}^V = g_{d_{ii}}^V \equiv g_{\text{SM}} \quad \text{and} \quad g_{u_{ii}}^A = g_{d_{ii}}^A = 0 \quad (4)$$

and

$$g_{X_D}^V = 0 \quad \text{and} \quad g_{X_D}^A \equiv g_X \quad (5)$$

$$g_{u_{ii}}^V = g_{d_{ii}}^V = 0 \quad \text{and} \quad g_{u_{ii}}^A = g_{d_{ii}}^A \equiv g_{\text{SM}}, \quad (6)$$

respectively, where we assume quark couplings to the mediator are the same for all the flavours and set all flavour off-diagonal couplings to zero. With this simplification of a single universal coupling for the SM- Y_1 interactions, the model has only four independent parameters, *i.e.* two couplings and two masses:

$$\{g_{\text{SM}}, g_X, m_X, m_Y\}. \quad (7)$$

We note that the mediator width is calculated from the above parameters. In the following sections, we take $g_{\text{SM}} = 1$ and $g_X = 0.25$ as our benchmark for the vector and axial-vector mediator scenario [33, 39].

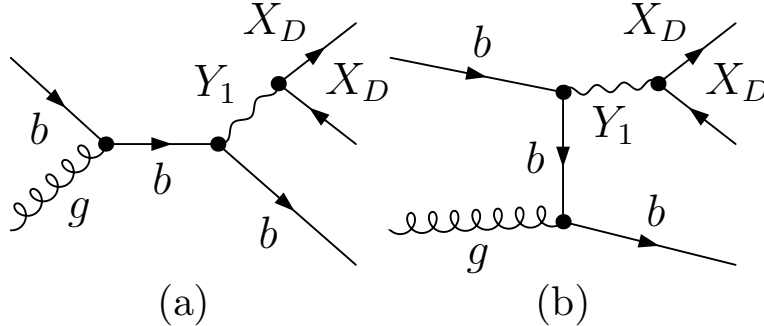


FIG. 1. The LO Feynman diagrams for the process $pp \rightarrow X_D \bar{X}_D + b + X$ at the LHC.

As we know, the cross section for the partonic process $g(p_1) + b(p_2) \rightarrow X_D(k_3) \bar{X}_D(k_4) + b(k_5)$ should be the same as that for its charge conjugate subprocess $g(p_1) + \bar{b}(p_2) \rightarrow X_D(k_3) \bar{X}_D(k_4) + \bar{b}(k_5)$, and the luminosity of the bottom quark in a proton is same as the anti-bottom quark. Therefore, the production rates of the $X_D \bar{X}_D b$ and the $X_D \bar{X}_D \bar{b}$ are identical at the LHC. In the following sections, we denote that the parent process $p + p \rightarrow X_D \bar{X}_D + b + X$ includes the two partonic process above unless otherwise indicated. There are two Feynman diagrams for this process at leading order(LO), which are shown in Fig.1. In our calculation, the mediator width is automatically computed by using the MadWidth module for each parameter point. The above benchmark coupling strength leads to $\Gamma_Y/m_Y \sim 0.05$ for $m_Y > 2m_X$ and $\Gamma_Y/m_Y \sim 0.025$ for $m_Y < 2m_X$ both for the vector and axial-vector mediators. Our calculation and simulation are based on the framework of MADGRAPH5_AMC@NLO [46]. The one-loop QCD corrections are computed using the program MADLOOP [47] which is based on the OPP method [48, 49]. The ultraviolet divergences and rational R_2 terms are calculated automatically using the NLOCT package [50] and the infrared subtraction terms for real emissions are generated by MADFKS [51]. Event generation is obtained by matching short-distance events to the parton shower using the MC@NLO framework [52], which is implemented for Pythia6 [53]. We define all jets, including b-jet, using the anti- k_T algorithm as implemented in FastJet with the jet cone radius $R = 0.4$. Additionally, we require $p_T(j) > 15 \text{ GeV}$ and $\eta(j) < 4.5$ for all jets in the event. The b-jets, originating from b-quarks, are defined as the long lifetime and the large

	$X_D\overline{X}_D j$	$X_D\overline{X}_D \gamma$	$X_D\overline{X}_D b$	$X_D\overline{X}_D Z$	$X_D\overline{X}_D W^\pm$
$\sigma(pb)$	8.245 ± 0.053	$0.1202 \pm 9.0\text{e-}4$	$0.1019 \pm 1.5\text{e-}3$	$0.04616 \pm 1.2\text{e-}4$	$4.796\text{e-}3 \pm 1.3\text{e-}5$

TABLE I. The NLO cross sections for DM pair production in association with a visible particle for the vector mediator at the 13 TeV LHC with the coupling parameters $g_X = 1$ and $g_{\text{SM}} = 0.25$.

mass of b hadrons.

III. NUMERICAL RESULTS AND DISCUSSION

A. Total cross section

In this section we provide LO and NLO QCD predictions for the total cross sections for the process $pp \rightarrow X_D\overline{X}_D + b + X$ at the 13 TeV LHC. We take NN23LO1 and NN23NLO PDF sets [54] for LO and NLO calculations, and the corresponding fitted values $\alpha_s(M_Z) = 0.130$ and $\alpha_s(M_Z) = 0.118$ are used for the LO and NLO calculations, respectively. The central value μ_0 for the renormalisation (μ_R) and factorisation (μ_F) scales is set to $H_T/2$, where $H_T = \sum_i \sqrt{p_{T,i}^2 + m_i^2}$, which is the sum of the transverse momenta of all final-state particles. The scale uncertainty is estimated by varying the scales μ_R and μ_F , from $\mu_0/2$ to $2\mu_0$, independently.

In table I, we list the total cross sections of dark matter associated with various visible particles production at 13 TeV LHC, which is obtained with `MADGRAPH5_AMC@NLO`. For all the jets, including b-jet, we set the distance in the (η, ϕ) plane $R = 0.4$, $p_T(j) > 15 \text{ GeV}$ and $\eta(j) < 4.5$. For the process $pp \rightarrow X_D\overline{X}_D + \gamma + X$, we set the $p_T(\gamma) > 20 \text{ GeV}$. For the process $pp \rightarrow X_D\overline{X}_D W^\pm + X$ and $pp \rightarrow X_D\overline{X}_D Z + X$, we don't consider the W^\pm and Z subsequent decay and add any select cuts. We find that the cross section of $pp \rightarrow X_D\overline{X}_D + b + X$ is comparable with the process $pp \rightarrow X_D\overline{X}_D + \gamma + X$, much larger than the process $pp \rightarrow X_D\overline{X}_D W^\pm + X$ and $pp \rightarrow X_D\overline{X}_D Z + X$. If considering the W and Z boson subsequent leptonic or hadronic decay, the cross section for the process $pp \rightarrow X_D\overline{X}_D W^\pm + X$ and $pp \rightarrow X_D\overline{X}_D Z + X$ will be even smaller.

In Fig.2, we present the DM mass dependence of the cross sections and the corresponding K-factors for the $pp \rightarrow X_D\overline{X}_D + b + X$ process induced by the vector, axial-vector mediator by taking $M_Y = 1000 \text{ GeV}$ at 13TeV LHC, separately. The dependence on the renormalization

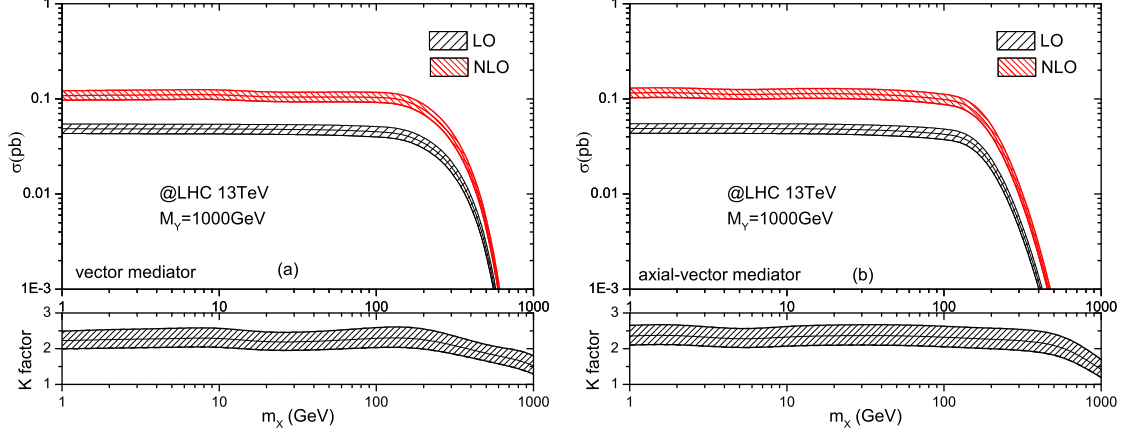


FIG. 2. The LO, NLO QCD corrected integrated cross sections and the corresponding K -factors as the functions of the DM mass for the process $pp \rightarrow X_D \bar{X}_D + b + X$ at the 13 TeV LHC with $M_Y = 1000$ GeV and $\mu = \mu_0$, the shaded band represents the deviation from this scale when the scales vary from $\mu_0/2$ to $2\mu_0$.

and factorization scales, with the simplification $\mu = \mu_r = \mu_f$, is illustrated by the shaded band linking the predictions obtained at $\mu = 2\mu_0$ and $\mu = 1/2\mu_0$, while the central scale choice $\mu = \mu_0$ is illustrated by the curve inside the shaded band. As shown in the figures, the cross sections are insensitive to the DM mass m_X in the range of $m_X < 100$ GeV, and start to decrease rapidly with the increment of m_X when $m_X > 100$ GeV. This is due to the final state phase space reduced rapidly when the dark matter mass m_X increasing. We find that the contributions from the vector-mediator and axial-vector-mediator can not be distinguished until $m_X > 100$ GeV. The scale uncertainties are not significantly reduced when comparing the LO and NLO QCD predictions. We define the K -factor as $K(\mu) = \sigma^{(NLO)}(\mu)/\sigma^{(LO)}(\mu_0)$ and find that the K -factors are more than 2 at lower mediator mass for both the vector and axial-vector mediators.

In Fig.3, we show that the vector and axial-vector mediators mass dependence of the LO, NLO QCD corrected integrated cross sections and the corresponding K -factor for the process $pp \rightarrow X_D \bar{X}_D + b + X$ at the 13 TeV LHC with $m_X = 10$ GeV. The dependence on the renormalization and factorization scales is illustrated by the shaded band linking the predictions obtained at $\mu = 2\mu_0$ and $\mu = 1/2\mu_0$ with the simplification $\mu = \mu_r = \mu_f$, and the central scale choice $\mu = \mu_0$ is illustrated by the curve inside the shaded band. When the vector and axial-vector mediators mass varies from 10 GeV to 1000 GeV, the NLO QCD

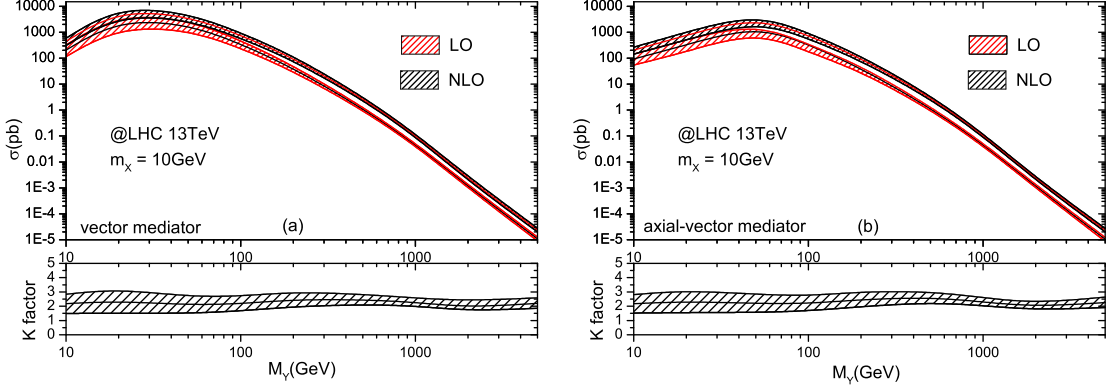


FIG. 3. The LO, NLO QCD corrected integrated cross sections and the corresponding K -factors as the functions of the vector mediator mass for the process $pp \rightarrow X_D \bar{X}_D + b + X$ at the 13TeV LHC with $m_X = 10 \text{ GeV}$ with the default scale $\mu = \mu_0$, the shaded band represents the deviation from this scale when the scales vary from $\mu_0/2$ to $2\mu_0$.

corrections modify the LO cross sections obviously. The similar behavior is demonstrated in the monojet production at the LHC [35]. The vector and axial-vector DM mediators show similar behaviour in terms of K -factors and scale dependence. This is because that in the massless limit the only terms which are sensitive to the axial nature of the coupling are the four-quark amplitudes, which is a small part of the total NLO cross section. The total cross sections and K -factors of some benchmark points are shown in table II.

B. Kinematic distributions

In order to obtain observable results in physics, we need to consider the parton-shower effects for the process $pp \rightarrow X_D \bar{X}_D + b + X$. We use Pythia6 to perform the parton-shower simulations. In Fig.4, we provide the differential distributions and the corresponding K factors of transverse momenta p_T and rapidity y for the hardest jet(j1) and hardest b-jet(b1), the distance in the (η, ϕ) plane R between the hardest jet(j1) and hardest b-jet(b1), and the missing transverse momenta E_T^{miss} at 13TeV LHC with $m_Y = 1000 \text{ GeV}$ and $m_X = 10 \text{ GeV}$ for vector mediator. For the p_T differential distributions of the hardest b-jet(b1) in Fig.4(a), the NLO QCD correction enhance the LO results at all region significantly, especially at lower p_T regions, the K -factor can reach about 3. In Fig.4(b) and (d), we present the

$(m_Y, m_X)[GeV]$	vector mediator			axial-vector mediator		
	LO(pb)	NLO(pb)	K-factor	LO(pb)	NLO(pb)	K-factor
(10,1)	1.778e4 \pm 58	6.744e4 \pm 790	3.772	1.733e4 \pm 56	6.449e4 \pm 55	3.721
(10,10)	204.8 \pm 0.7	443.5 \pm 5	2.166	94.24 \pm 0.34	196.5 \pm 2.2	2.085
(100,1)	361.5 \pm 1.6	861.2 \pm 9.3	2.382	361 \pm 1.8	886.4 \pm 8.9	2.455
(100,10)	362.5 \pm 1.7	841.1 \pm 8.4	2.320	348.1 \pm 1.6	848.5 \pm 9.7	2.438
(100,100)	0.365 \pm 1.3e-3	0.9901 \pm 8.8e-3	2.713	0.114 \pm 3.5e-4	0.2974 \pm 6.3e-3	2.609
(500,10)	1.186 \pm 5.3e-3	2.695 \pm 3.1e-2	2.272	1.23 \pm 5e-3	3.572 \pm 3.7e-2	2.904
(500,100)	1.132 \pm 4.7e-3	3.245 \pm 3.9e-2	2.867	1.005 \pm 4e-3	2.746 \pm 0.031	2.732
(1000,10)	4.836e-2 \pm 2e-4	0.1019 \pm 1.5e-4	2.107	4.91e-2 \pm 2.2e-4	0.1173 \pm 1.4e-3	2.390
(1000,100)	4.588e-2 \pm 2e-4	0.1296 \pm 1.5e-3	2.825	4.35e-2 \pm 1.9e-4	0.1138 \pm 1.32e-3	2.616
(1000,500)	9.069e-3 \pm 3.2e-5	2.684e-2 \pm 6.2e-4	2.960	5.4e-4 \pm 2e-6	1.21e-3 \pm 1.2e-5	2.241
(1000,1000)	2.53e-6 \pm 8.2e-9	4.91e-6 \pm 7.8e-8	1.941	4.77e-7 \pm 1.4e-9	6.705e-7 \pm 6.7e-9	1.406

TABLE II. LO and NLO QCD cross sections and corresponding K factors for DM pair production in association with a b-jet for the vector and axial-vector mediators at the 13TeV LHC. Several benchmark points for the vector and axial-vector mediators and DM masses are presented with the coupling parameters $g_X = 1$ and $g_{SM} = 0.25$.

hardest jet(j1) p_T and y differential distributions. We find that the K-factors are about 2 at all regions. The hardest jet(j1) transverse momentum distribution exhibit a plateau extending up to half the vector mediator mass, which is due to that it could alternatively originate directly from the vector mediator decay, the similar behavior also occurs in Ref.[55]. For the rapidity differential distributions for the hardest b-jet(b1) in Fig.4(c), the NLO QCD correction is very large at high rapidity. In Fig.4(e), the missing E_T distribution is displayed, we can see that the NLO QCD correction effect is not obvious, especially at large E_T^{miss} . Due to the uncertainty of numerical integration, the K-factor is not stable at large E_T^{miss} region. For the differential distributions of the distance in the (η, ϕ) plane R between the hardest jet(j1) and hardest b-jet(b1) in Fig.4(f), we find that there is a bump from 0.7 to 1.5, and the NLO correction enhance the LO results significantly at this region.

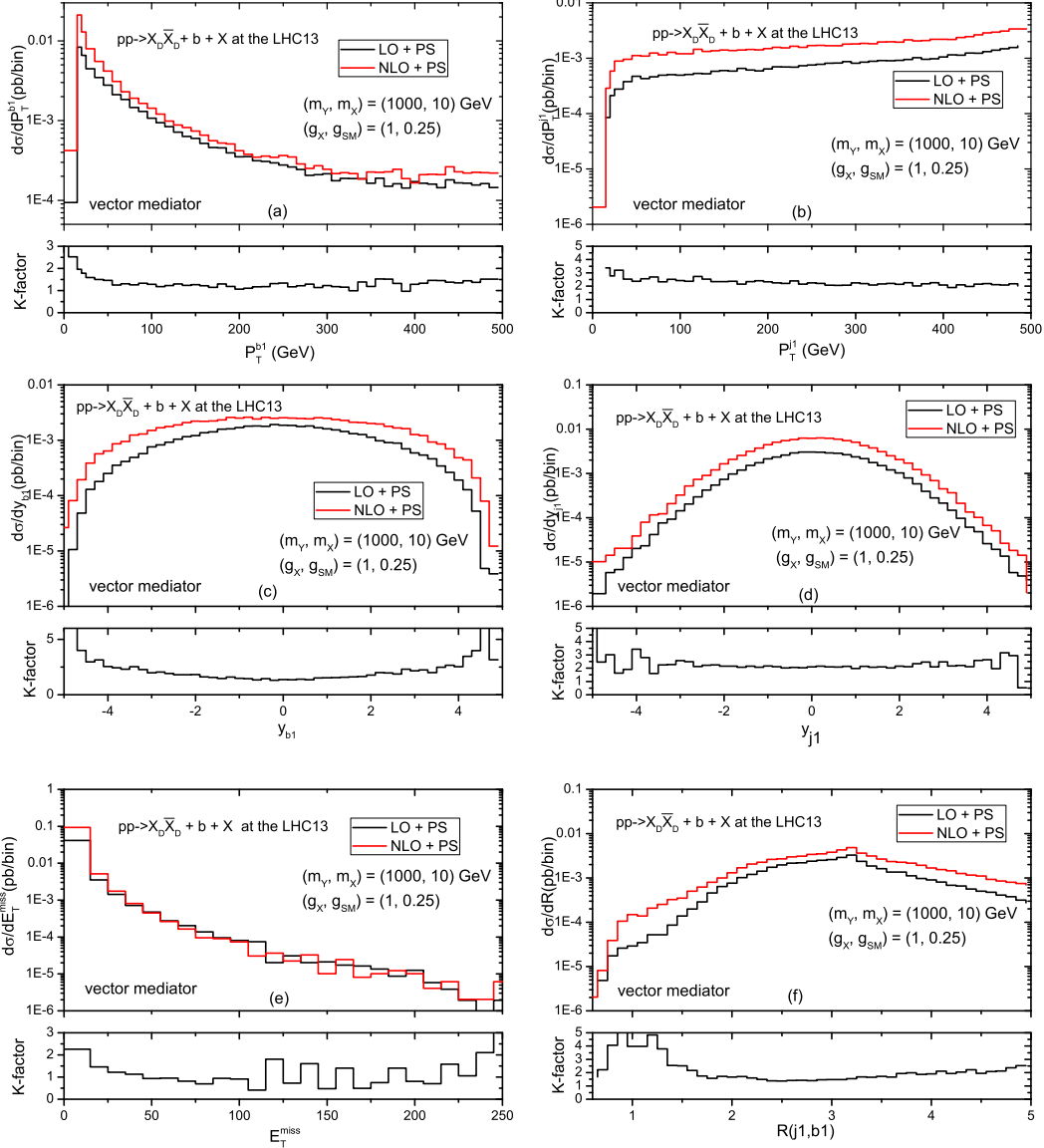


FIG. 4. The LO, NLO QCD corrected distributions and corresponding K factors of the transverse momenta and rapidity of the hardest jet(j1), hardest b-jet(b1), the distributions of missing transverse momenta E_T^{miss} and distance in the (η, ϕ) plane R between the hardest jet(j1) and hardest b-jet(b1) for the $pp \rightarrow X_D \bar{X}_D + b + X$ processes at the $\sqrt{s} = 13\text{TeV}$ LHC.

C. Discovery potential for the $X_D \bar{X}_D + b$ production at the 13TeV LHC

In this section, we study the discovery potential for the signal of $X_D \bar{X}_D + b$ production at the 13TeV LHC. In general, the cross section for the process $pp \rightarrow X_D \bar{X}_D + b + X$ is a function of the relevant couplings, the DM mass and the mediator mass. We know that there are more advantages in looking for relative light dark matter particles on the colliders than

on the direct and indirect experiments. From Fig.2, we can see that the total cross sections have barely changed in the range of light mediator mass, and they are almost same for the vector and axial-vector mediators. Thus, we choose vector mediator mass $m_X = 10 \text{ GeV}$ as the characteristic parameter. The significance of signal over background S is defined as

$$S = \frac{N_S}{\sqrt{N_B}} = \frac{\sigma_S \sqrt{\mathcal{L}}}{\sqrt{\sigma_B}}, \quad (8)$$

where $N_{S,B}$ and $\sigma_{S,B}$ are the event numbers and cross sections for signal and background, and \mathcal{L} denotes the integrated luminosity. The SM background mainly comes from the processes $pp \rightarrow Z + b$ and $pp \rightarrow Z + \bar{b}$ ($Z \rightarrow \nu\bar{\nu}$, $\nu = \nu_e, \nu_\mu, \nu_\tau$), where the neutrino is also the missing energy. Using the same selection cuts as the signal, we obtain the LO cross section at 13TeV LHC as: $\sigma = 125.2 \pm 0.1232 \text{ (pb)}$. If considering the NLO QCD correction, the total cross section is equal to the LO cross-section multiplying a K-factor about 1.25 [56]. In Fig.5, we present the 5σ discovery and 3σ exclusion limits for the $X_D \bar{X}_D + b$ production at the 13 TeV LHC. If no signal events will have been detected after accumulating an integrated luminosity of 116 fb^{-1} , then the region with mediator mass $M_Y < 1000 \text{ GeV}$ can be excluded at the 3σ level. On the other hand, if the mediator mass satisfies $M_Y < 1000 \text{ GeV}$, then the signal $X_D \bar{X}_D + b$ is going to be discovered at the 5σ level before accumulating an integrated luminosity of 323 fb^{-1} . This result shows that there is a more strong potential ability to distinguish dark matter particles than the mono- Z productions [39].

IV. SUMMARY

The LHC provides an ideal facility to search for DM particles. Accurate and precise predictions for DM associated production rates and distributions are necessary to obtain robust constraints on different DM models. In this paper, we calculated a pair of fermionic dark matter particles associated production with a b-jet at the LHC, including next-to-leading order(NLO) QCD corrections and parton-shower effects. We have considered a simplified model where DM is a Dirac fermion and couples to the SM via either a vector or axial-vector mediator. For the $X_D \bar{X}_D + b$ production in the vector and axial-vector mediator models, our results show that higher-order corrections have a significant effect both on the overall production rate as well as on the shape of differential distributions. The NLO QCD corrections to the LO production rates can be very large, the K factors can reach to 3 in

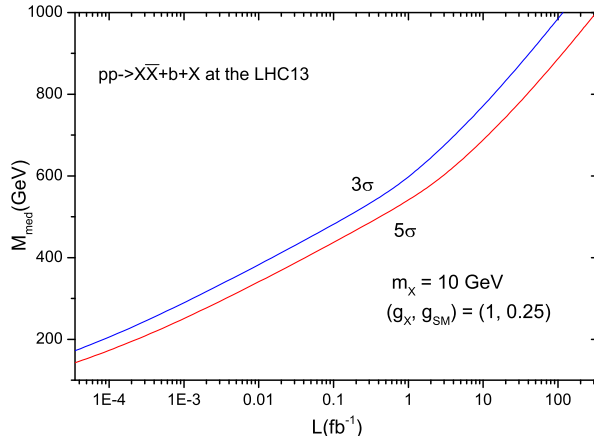


FIG. 5. 5σ discovery and 3σ exclusion limits for the process $pp \rightarrow X_D \bar{X}_D + b + X$ at the 13 TeV LHC with the coupling parameters $g_X = 1$ and $g_{SM} = 0.25$. If a discovery is made, then the regions below the red line is favored. If no signal is found, then the region above the blue line is excluded.

reasonable parameter space. This shows that the NLO corrections have a noticeable impact on the DM + b-jet signal and must be considered. We also considered the discovery potential for this process, and found that this process has potential to be detected at the LHC.

V. ACKNOWLEDGMENTS

This work was supported by the National Natural Science Foundation of China (No.11205003, No.11305001, No.11575002).

-
- [1] G. Bertone, D. Hooper and J. Silk, “Particle dark matter: Evidence, candidates and constraints,” *Phys. Rept.* **405** (2005) 279, [hep-ph/0404175].
 - [2] J. L. Feng and J. Kumar, “The WIMPless Miracle: Dark-Matter Particles without Weak-Scale Masses or Weak Interactions,” *Phys. Rev. Lett.* **101** (2008) 231301, [arXiv:0803.4196].
 - [3] S.P. Martin, “A Supersymmetry primer”, In *Kane, G.L. (ed.): Perspectives on supersymmetry II* 1-153, [hep-ph/9709356].
 - [4] M. Drees, R. Godbole, and P. Roy, “Theory and phenomenology of sparticles: An account of four-dimensional N=1 supersymmetry in high energy physics”.

- [5] T. Appelquist, H.-C. Cheng and B.A. Dobrescu, “Bounds on universal extra dimensions”, Phys. Rev. **D64** (2001) 035002, [hep-ph/0012100].
- [6] N. Arkani-Hamed, A.G. Cohen and H. Georgi, “Electroweak symmetry breaking from dimensional deconstruction”, Phys. Lett. **B513** (2001) 232, [hep-ph/0105239].
- [7] L. Wu, B. Yang and M. Zhang, “A Lower Bound on the Mass of Little Higgs Dark Matter after PandaX-II/LUX 2016 and LHC Run-1,” arXiv:1607.06355 [hep-ph].
- [8] R. Bernabei *et al.* [DAMA and LIBRA Collaborations], “New results from DAMA/LIBRA,” Eur. Phys. J. C **67** (2010) 39, [arXiv:1002.1028].
- [9] CoGeNT Collaboration, C. Aalseth, P. Barbeau, J. Colaresi, J. Collar, J. Diaz Leon, *et al.*, “Search for an Annual Modulation in a P-type Point Contact Germanium Dark Matter Detector”, Phys. Rev. Lett. **107** (2011) 141301, [arXiv:1106.0650]
- [10] CRESST Collaboration, G. Angloher *et al.*, “Results from 730 kg days of the CRESST-II Dark Matter Search”, Eur. Phys. J. **C 72** (2012) 1971, [arXiv:1109.0702].
- [11] CDMS Collaboration, R. Agnese *et al.*, “Silicon Detector Dark Matter Results from the Final Exposure of CDMS II”, Phys. Rev. Lett. **111** (2013) 251301, [arXiv:1304.4279].
- [12] E. Aprile *et al.* [XENON100 Collaboration], “Dark Matter Results from 225 Live Days of XENON100 Data,” Phys. Rev. Lett. **109** (2012) 181301, [arXiv:1207.5988].
- [13] D. S. Akerib *et al.* [LUX Collaboration], “First results from the LUX dark matter experiment at the Sanford Underground Research Facility,” Phys. Rev. Lett. **112** (2014) 091303, [arXiv:1310.8214].
- [14] SuperCDMS Collaboration, R. Agnese *et al.*, Phys. Rev. Lett. **112**, 241302 (2014), [1402.7137].
- [15] Y. G. Kim and S. Shin, “Singlet Fermionic Dark Matter explains DAMA signal,” JHEP **0905**, 036 (2009) [arXiv:0901.2609].
- [16] A. L. Fitzpatrick, D. Hooper and K. M. Zurek, “Implications of CoGeNT and DAMA for Light WIMP Dark Matter,” Phys. Rev. D **81** (2010) 115005 [arXiv:1003.0014].
- [17] J. Kopp, T. Schwetz and J. Zupan, “Global interpretation of direct Dark Matter searches after CDMS-II results,” JCAP **1002**, 014 (2010) [arXiv:0912.4264].
- [18] E. Kuflik, A. Pierce and K. M. Zurek, “Light Neutralinos with Large Scattering Cross Sections in the Minimal Supersymmetric Standard Model,” Phys. Rev. D **81** (2010) 111701 [arXiv:1003.0682].

- [19] S. Andreas, C. Arina, T. Hambye, F. -S. Ling and M. H. G. Tytgat, “A light scalar WIMP through the Higgs portal and CoGeNT,” *Phys. Rev. D* **82** (2010) 043522 [arXiv:1003.2595].
- [20] S. Chang, J. Liu, A. Pierce, N. Weiner and I. Yavin, “CoGeNT Interpretations,” *JCAP* **1008** (2010) 018 [arXiv:1004.0697].
- [21] R. Essig, J. Kaplan, P. Schuster and N. Toro, “On the Origin of Light Dark Matter Species,” [arXiv:1004.0691].
- [22] H. An, S. L. Chen, R. N. Mohapatra, S. Nussinov and Y. Zhang, “Energy Dependence of Direct Detection Cross Section for Asymmetric Mirror Dark Matter,” *Phys. Rev. D* **82**, 023533 (2010) [arXiv:1004.3296].
- [23] V. Barger, M. McCaskey and G. Shaughnessy, “Complex Scalar Dark Matter vis-à-vis CoGeNT, DAMA/LIBRA and XENON100,” *Phys. Rev. D* **82** (2010) 035019 [arXiv:1005.3328].
- [24] D. Hooper, J. I. Collar, J. Hall, D. McKinsey and C. Kelso, “A Consistent Dark Matter Interpretation For CoGeNT and DAMA/LIBRA,” *Phys. Rev. D* **82** (2010) 123509 [arXiv:1007.1005].
- [25] CDF Collaboration, “A Search for dark matter in events with one jet and missing transverse energy in $p\bar{p}$ collisions at $\sqrt{s} = 1.96$ TeV,” *Phys. Rev. Lett.* **108**, 211804 (2012), [arXiv:1203.0742].
- [26] G. Aad *et al.* [ATLAS Collaboration], “Search for dark matter candidates and large extra dimensions in events with a jet and missing transverse momentum with the ATLAS detector”, [arXiv:1210.4491].
- [27] S. Chatrchyan *et al.* [CMS Collaboration], “Search for dark matter and large extra dimensions in monojet events in pp collisions at $\sqrt{s} = 7$ TeV”, *JHEP* **1209**, 094 (2012), [arXiv:1206.5663].
- [28] G. Aad *et al.* [ATLAS Collaboration], “Search for dark matter candidates and large extra dimensions in events with a photon and missing transverse momentum in pp collision data at $\sqrt{s} = 7$ TeV with the ATLAS detector”, [arXiv:1209.4625].
- [29] S. Chatrchyan *et al.*, [CMS Collaboration], “Search for Dark Matter and Large Extra Dimensions in pp Collisions Yielding a Photon and Missing Transverse Energy”, *Phys. Rev. Lett.* **108**, 261803 (2012), [arXiv:1204.0821].
- [30] The ATLAS collaboration, “Search for dark matter pair production in events with a hadronically decaying W or Z boson and missing transverse momentum in pp collision data at $\sqrt{s} = 8$

- TeV with the ATLAS detector”, ATLAS-CONF-2013-073.
- [31] CMS Collaboration [CMS Collaboration], “Search for dark matter in the mono-lepton channel with pp collision events at center-of-mass energy of 8 TeV ”, CMS-PAS-EXO-13-004.
 - [32] G. Aad *et al.*, [ATLAS Collaboration], “Search for dark matter in events with a hadronically decaying W or Z boson and missing transverse momentum in pp collisions at $\sqrt{s}=8$ TeV with the ATLAS detector”, [arXiv:1309.4017].
 - [33] M. Backovic, M. Kramer, F. Maltoni, A. Martini, K. Mawatari and M. Pellen, “Higher-order QCD predictions for dark matter production at the LHC in simplified models with s-channel mediators,” *Eur. Phys. J. C* **75** (2015) no.10, 482 [arXiv:1508.05327].
 - [34] U. Haisch, F. Kahlhoefer and J. Unwin, “The impact of heavy-quark loops on LHC dark matter searches”, *JHEP* **1307** (2013) 125, [arXiv:1208.4605].
 - [35] P.J. Fox and C. Williams, “Next-to-Leading Order Predictions for Dark Matter Production at Hadron Colliders”, *Phys. Rev.* **D87** (2013) 054030, [arXiv:1211.6390].
 - [36] F.-P. Huang, C.-S. Li, J. Wang and D.-Y. Shao, “Searching for the signal of dark matter and photon associated production at the LHC beyond leading order”, *Phys. Rev.* **D87** (2013) 094018, [arXiv:1210.0195].
 - [37] J. Wang, C. S. Li, D. Y. Shao and H. Zhang, “Next-to-leading order QCD predictions for the signal of Dark Matter and photon associated production at the LHC,” *Phys. Rev. D* **84** (2011) 075011 [arXiv:1107.2048].
 - [38] U. Haisch, F. Kahlhoefer and E. Re, “QCD effects in mono-jet searches for dark matter,” *JHEP* **1312** (2013) 007 [arXiv:1310.4491].
 - [39] M. Neubert, J. Wang and C. Zhang, “Higher-Order QCD Predictions for Dark Matter Production in Mono-Z Searches at the LHC,” *JHEP* **1602** (2016) 082 [arXiv:1509.05785].
 - [40] U. Haisch, F. Kahlhoefer and T. M. P. Tait, “On Mono-W Signatures in Spin-1 Simplified Models,” *Phys. Lett. B* **760** (2016) 207 [arXiv:1603.01267].
 - [41] O. Mattelaer and E. Vryonidou, “Dark matter production through loop-induced processes at the LHC: the s-channel mediator case,” *Eur. Phys. J. C* **75** (2015) no.9, [arXiv:1508.00564].
 - [42] N. Chen, Z. Kang and J. Li, arXiv:1608.00421 [hep-ph].
 - [43] T. Lin, E. W. Kolb and L. T. Wang, “Probing dark matter couplings to top and bottom quarks at the LHC,” *Phys. Rev. D* **88** (2013) no.6, 063510 [arXiv:1303.6638].

- [44] A. Alloul, N. D. Christensen, C. Degrande, C. Duhr and B. Fuks, “FeynRules 2.0 - A complete toolbox for tree-level phenomenology,” *Comput. Phys. Commun.* **185** (2014) 2250, [arXiv:1310.1921].
- [45] <http://feynrules.irmp.ucl.ac.be/wiki/DMSimp>.
- [46] J. Alwall, R. Frederix, S. Frixione, V. Hirschi, F. Maltoni, et al., *The automated computation of tree-level and next-to-leading order differential cross sections, and their matching to parton shower simulations*, *JHEP* **1407** (2014) 079, [arXiv:1405.0301].
- [47] V. Hirschi, R. Frederix, S. Frixione, M. V. Garzelli, F. Maltoni, and R. Pittau, *Automation of one-loop QCD corrections*, *JHEP* **05** (2011) 044, [arXiv:1103.0621].
- [48] G. Ossola, C. G. Papadopoulos, and R. Pittau, *Reducing full one-loop amplitudes to scalar integrals at the integrand level*, *Nucl. Phys.* **B763** (2007) 147–169, [hep-ph/0609007].
- [49] G. Ossola, C. G. Papadopoulos, and R. Pittau, *CutTools: A Program implementing the OPP reduction method to compute one-loop amplitudes*, *JHEP* **03** (2008) 042, [arXiv:0711.3596].
- [50] C. Degrande, *Automatic evaluation of UV and R₂ terms for beyond the Standard Model Lagrangians: a proof-of-principle*, [arXiv:1406.3030].
- [51] R. Frederix, S. Frixione, F. Maltoni, and T. Stelzer, *Automation of next-to-leading order computations in QCD: The FKS subtraction*, *JHEP* **10** (2009) 003, [arXiv:0908.4272].
- [52] S. Frixione and B. R. Webber, *Matching NLO QCD computations and parton shower simulations*, *JHEP* **06** (2002) 029, [hep-ph/0204244].
- [53] T. Sjostrand, S. Mrenna, and P. Z. Skands, *PYTHIA 6.4 Physics and Manual*, *JHEP* **05** (2006) 026, [hep-ph/0603175].
- [54] **NNPDF** Collaboration, R. D. Ball, V. Bertone, S. Carrazza, L. Del Debbio, S. Forte, A. Guffanti, N. P. Hartland, and J. Rojo, *Parton distributions with QED corrections*, *Nucl. Phys.* **B877** (2013) 290–320, [arXiv:1308.0598].
- [55] B. Fuks and H. S. Shao, “QCD next-to-leading order predictions matched to parton showers for vector-like quark models,” arXiv:1610.04622 [hep-ph].
- [56] J. M. Campbell, R. K. Ellis, F. Maltoni and S. Willenbrock, “Associated production of a Z Boson and a single heavy quark jet,” *Phys. Rev. D* **69** (2004) 074021 [hep-ph/0312024].